

### 3. Finite-Element Models

#### 3.1 Introduction

This chapter will be concerned with the finite-element approach to storm surges and tides. Compared with the finite-difference methods, the finite-element methods are more recent (they began to appear in the literature in the middle 1960s) but they are better suited for representing the topography realistically than are regular-grid finite-difference techniques.

Following WANG and CONNOR (1975a), the literature on finite-element methods will be briefly reviewed. Unlike in the finite-difference method, in the finite element method the variables satisfying the governing equations and boundary conditions are approximated by piecewise polynomials. The main advantage of the finite-element method is the highly flexible grid so that real water bodies can be modeled more realistically.

WANG and CONNOR (1975a) distinguished between the finite-element method and the discrete-element method as follows. The discrete-element method makes use of both the finite difference and finite-element methods. The discrete-element method, rather than using differential equations for the infinitesimal element, one can perform all the balances on the computational discrete element which can have an arbitrary shape. However, one generally uses square, rectangular, or triangular elements. In an element the variation of any given parameter is represented by discrete nodal values. Usually, these nodes are located at the center of the sides of the elements. To satisfy conservation, the discrete equation must approximate the differential equations as the control volume is reduced to zero. This may be difficult to prove for odd-shaped elements. SIMON-TOV (1974) and ERASLAN (1974) gave some examples of the discrete-element method. WANG and CONNOR (1975a) pointed out that one drawback of the discrete-element method is that if one wants to refine the grid at one point, e.g.  $(x_0, y_0)$ , then one must have the same value of  $\Delta x$  for all the elements along the line  $y = x_0$  and the same value of  $\Delta y$  for all elements along the line  $x = y_0$ . However, this is not a serious shortcoming, because either an interpolation technique or trapezoidally shaped elements can be developed to get around this problem.

According to WANG and CONNOR (1975a) the finite-element method was first used in 1956 in aeronautics. Until the late 1960s its use was mainly confined to solid and structural mechanics (ZIENKEWICZ, 1971). In the early stages the success of the finite-element method dependent on the existence of a variational statement of the problem. However, FINLAYSON and SCRIVEN (1965) showed that Galerkin's method can be derived from the method of weighted residuals and there is no need for a variational statement.

Consider the differential equation

$$Lu = f_0 \quad (3.1)$$

where,  $L$  is a differential operator,  $u$  is an exact solution, and  $f_0$  is the inhomogeneous term. Define the residual  $R$  as

$$R = L\hat{u} - f_0 \quad (3.2)$$

Application of a weighting function  $w$  to the residual and summation over the complete domain  $\Omega$  gives

$$WR = \int_{\Omega} R w d\omega = \int_{\Omega} (L\hat{u} - f_0) w d\omega \quad (3.3)$$

where, WR is the weighted residual. The finite-element solution is based on the condition that the weighted residual should vanish.

For some application of the finite-element method to circulation in shallow water bodies, see GALLAGHER and CHAN (1973), who calculated the steady wind driven circulation in shallow lakes under the rigid lid approximation. TAYLOR and DAVIS (1972) used a fourth-order predictor-corrector method for the time integration. They compared the trapezoidal rule and the finite elements in time. GROTKOP (1973) studied the same problem using linear finite elements in time. According to WANG and CONNOR (1975a) this method is less accurate than the trapezoidal rule. Consider the equation

$$M \dot{\tilde{x}} = F \quad (3.4)$$

where the tilde denotes a matrix quantity. Applying the linear finite elements in time to this equation gives the following recurrence relation:

$$M \tilde{x}_{n+1} = M \tilde{x}_n + \Delta t \left( \frac{1}{3} F_n + \frac{2}{3} F_{n+1} \right) \quad (3.5)$$

On the other hand, the trapezoidal rule can be written as

$$M \tilde{x}_{n+1} = M \tilde{x}_n + \frac{\Delta t}{2} (F_n + F_{n+1}) \quad (3.6)$$

Note that the trapezoidal form is centered around time  $n + 1/2$  and is better than the skewed form (eq. 3.5). TAYLOR and DAVIS (1972) made use of a cubic expansion in time based on trial runs. It should be noted that the predictor-corrector method and the cubic finite-element method give more accurate results than the trapezoidal rule; however, they require much more computational effort. Because of asymmetric matrices, even the trapezoidal rule is not very efficient.

NORTON et al. (1973) used the Newton-Raphson method including the nonlinear terms. WANG and CONNOR (1975a, 1975b) gave some new concepts, which helped to solve troublesome details encountered in an earlier studies. The boundary condition of nonzero slip in the tangential velocity field is conceptually difficult to apply when curved land boundaries are approximated by triangular elements. At the break points of the model boundary, the nonzero tangential velocity component gives rise to flow across the adjoining segments. Then, to satisfy the continuity equation at the break points, one is forced to equate both velocity components to zero. NORTON et al. (1973) suggested that one should keep as few break points as possible and these points both the velocity component must be prescribed equal to zero. Once one is forced to do this, the flexibility of the finite-element grid is sacrificed; also, near the break points one must use a fine grid. This will necessitate the use of the long and narrow triangles (distorted elements) WANG and CONNOR (1975a) resolved this problem by a proper definition of a normal direction at the break points, and this permits a nonzero tangential component of the velocity without reducing the number of break points.

For a detailed derivation of the equations involved in the finite-element method see WANG and CONNOR (1975a). They solved several simple problems to enable comparison with analytical solutions. Finally, they applied the technique to a study of tides in the Massachusetts Bay. WANG and CONNOR (1975a) also formulated a two-layer model (for other details see CONNOR and WANG [1973] and WANG and CONNOR [1975b]).

WEARE (1976) compared the computational expenses for the shallow-water problems using finite-difference and finite-element methods and concluded that, at present, finite-element methods are less economical due to the use of band algorithms. However, the situation is changing now. GRAY and PINDER (1976) made a comprehensive comparison of finite-difference and finite-element methods and showed that the finite-element representation of the differential equations is essentially a spatial average of standard finite-difference equations written for each mode of the grid.

KLEINSTREUER and HOLDEMAN (1980) developed an interactive triangular finite-element mesh generator for water bodies of the arbitrary geometry. NIEMEYER (1979a) applied a finite-element technique to study tidal flow in certain water bodies in Hawaii. ORLOB (1972) used triangular grids for studying circulation in the San Francisco Bay area, but he wrote the equation in finite-difference form. FIX (1975) used a finite-element model to study the circulation in a limited area of the mid-ocean.

GROTKOP (1973) used a finite-element technique for studying waves in the North Sea. CHENG (1972, 1974), CHENG et al. (1976), CHENG and TUNG (1970), GALLAGHER et al. (1973), GALLAGHER and CHAN (1973) and HUEBNER (1974) applied finite-element techniques to study wind-driven circulation in lakes. Other relevant works are those of CHENG (1978), WALTERS and CHENG (1980a, 1980b), JAMART and WINTER (1979), MEI and CHEN (1975), REICHARD and CELIKOL (1978), HAUGUEL (1978), LE PROVOST (1978), LEIMKUHLER et al. (1975), and TAYLOR and HOOD (1973).

JAMART and WINTER (1978) used the finite-element approach to study tidal propagation. One of their important assumptions is periodic motion. Because of this assumption, this model cannot be used to study storm surges (which are not periodic). KAWAHARA et al. (1977) used a mixed approach of the finite element method and perturbation method, again with the assumption of periodic motion. THACKER (1977) studied the normal modes in a circular basin using an irregular-grid finite difference model (this will be considered in detail below). WANG (1977) criticized Thacker's work and pointed that Thacker's model is unstable and inaccurate.

MEI and CHEN (1975) introduced a hybrid-element method for water problems in infinite fluid domain. They introduced artificial boundaries and thus divided the fluid into a finite-element region, in the neighborhood of infinity or of singular points. In the finite element region polynomial interpolating functions are used to approximately represent the unknown functions. In the super-element region, infinite series solutions are used. Numerical computations involve only integrals in a finite domain and the inversion of a banded symmetric matrix. Examples of shallow-water waves in a harbor are included.

HOUSTON (1978) used a finite-element numerical model to study the interaction of tsunamis with the Hawaiian Islands. This model solves the generalized Helmholtz equation:

$$\nabla[D(x, y)\nabla\phi(x, y)] + \frac{\omega^2}{g}\phi(x, y) = 0$$

where,  $\phi(x, y)$  is the velocity potential,  $\omega$  is the angular frequency, and  $D(x, y)$  is the water depth. This equation is not relevant for storm surge studies, at least in its present simple form.

### 3.2 Finite-Element Models for Tides and Storm Surges

BREBBIA and PARTRIDGE (1976) studied the tides and storm surges in the North Sea using two finite-element models. In both models they used six-noded triangular elements. One model made use of an implicit integration scheme with curved sides, and the other utilized an explicit integration scheme. The models are vertically integrated and include tides, wind stress, atmosphere pressure gradients, bottom friction, Coriolis force, and advection terms.

Following BREBBIA and PARTRIDGE (1976), a Cartesian coordinate system, with the origin at the equilibrium water level and the z-axis pointing upwards, is used. Let  $D(x, y)$  be the deviation of the free surface from its equilibrium position. The horizontal momentum equations can be written in the following form:

$$\frac{\partial u}{\partial t} + u \frac{\partial u}{\partial x} + v \frac{\partial u}{\partial y} = B \tag{3.7}$$

$$\frac{\partial v}{\partial t} + u \frac{\partial v}{\partial x} + v \frac{\partial v}{\partial y} = B$$

$$B_x = fv - g \frac{\partial h}{\partial x} - \frac{\partial}{\partial x} \left( \frac{P_a}{\rho} \right) + \frac{1}{\rho} \tau_{sx} - \frac{1}{\rho} \tau_{Bx} \tag{3.8}$$

$$B_y = fu - g \frac{\partial h}{\partial y} - \frac{\partial}{\partial y} \left( \frac{P_a}{\rho} \right) + \frac{1}{\rho} \tau_{sy} - \frac{1}{\rho} \tau_{By}$$

where,  $u$  and  $v$  the  $x$  and  $y$  components of the velocity field averaged in the vertical direction. The following expressions can be written for the surface stress,  $\tau_s$ , and the bottom stress,  $\tau_B$ ,

$$\tau_{s_i} = \frac{\gamma}{\rho} \frac{W_i}{H^2} (W_x^2 + W_y^2)^{1/2}, \quad i = x \text{ or } y \tag{3.9}$$

$$\tau_{B_i} = \frac{-g}{C^2} \rho \frac{V_i}{H} (u^2 + v^2)^{1/2}, \quad i = 1, 2$$

If  $i = 1, V_i = u$ ; if  $i = 2, V_i = v$ . Here,  $C$  is a Chezy coefficient,  $W_x$  and  $W_y$  are the  $x$  and  $y$  components of the wind, and  $\gamma$  is a parameter related to the atmospheric density,  $\rho_a$  ( $\gamma = \rho_a$ , constant). Finally,  $H = D + h$ .

The vertically integrated from of the continuity equation is

$$\frac{\partial H}{\partial t} + \frac{\partial}{\partial x} (Hu) + \frac{\partial}{\partial y} (Hv) = 0 \tag{3.10}$$

At closed boundaries, the velocity component perpendicular to the boundary is set to zero, while the tangential component is nonzero. At open boundaries, either the normal component of the velocity or the water level is prescribed.

To develop the finite-element model, two momentum equations and the continuity equation (3.10) together with the influx type boundary condition must be written in the following weighted residual manner:

$$\begin{aligned} \iint \left( \frac{\partial u}{\partial t} + u \frac{\partial u}{\partial x} - B_x \right) \delta u dA &= 0 \\ \iint \left( \frac{\partial v}{\partial t} + u \frac{\partial v}{\partial x} + v \frac{\partial v}{\partial y} - B_y \right) \delta v dA &= 0 \\ \iint \left[ \frac{\partial H}{\partial t} + \frac{\partial}{\partial x} (Hu) + \frac{\partial v}{\partial y} (Hv) \right] \delta H dA &= \int (H V_n - H \bar{V}_n) \delta H dS = \int H \bar{V}_n \delta H dS \end{aligned} \quad (3.11)$$

Where  $n$  denotes the normal and  $V_n$  denotes the component of the velocity. It will be assumed that over an element, the same interpolation for the unknown  $u$ ,  $v$ , and  $H$ . Thus

$$\begin{aligned} u &= \phi u^n \\ v &= \phi v^n \\ H &= \phi H^n \end{aligned} \quad (3.12)$$

where,  $\phi$  is the interpolation function and  $u^n$ ,  $v^n$ , and  $H^n$  are the nodal of  $u$ ,  $v$ , and  $H$ . A six-nodal triangular finite-element grid was used. These elements were referred to as "isoparametric" by BREBBIA and PARTRIDGE (1976). The advantage of using curved elements is the suppression of the spurious forces generated on the boundaries by straight-line segments joining at an angle (CONNOR and BREBBIA 1976).

From eq. (3.11) and (3.12)

$$\begin{aligned} M \frac{\partial u^n}{\partial t} + K u^n - f M v^n + G_x H^n + F_x &= 0 \\ M \frac{\partial v^n}{\partial t} + K v^n - f M u^n + G_y H^n + F_y &= 0 \\ M \frac{\partial H^n}{\partial t} + C_x u^n - C_y v^n + F_H &= 0 \end{aligned} \quad (3.13)$$

with the following definitions (superscript T denotes the transpose):

$$K = \int \frac{\partial}{\partial x} (\phi^T \phi) u dA + \int \frac{\partial}{\partial y} (\phi^T \phi) v dA + \frac{g}{C^2} \int \frac{\phi^T (u^2 + v^2)^{1/2}}{H} \phi dA$$

$$G_x = g \int \frac{\partial}{\partial x} (\phi^T \phi) dA$$

$$G_y = g \int \frac{\partial}{\partial y} (\phi^T \phi) v dA$$

$$M = \int \phi^T \phi dA$$

$$F_x = \int \phi^T \frac{\partial}{\partial x} \left( \frac{P_a}{\rho} \right) dA + \frac{\gamma}{\rho} \int \phi^T \frac{W_x}{H} (W_x^2 + W_y^2)^{1/2} dA$$

$$F_y = \int \phi^T \frac{\partial}{\partial y} \left( \frac{P_a}{\rho} \right) dA + \frac{\gamma}{\rho} \int \phi^T \frac{W_y}{H} (W_x^2 + W_y^2)^{1/2} dA$$

$$C_x = \int \frac{\partial}{\partial x} (\phi^T) H \phi dA$$

$$C_y = \int \frac{\partial}{\partial y} (\phi^T) H \phi dA$$

$$F_H = \int H \bar{V}_n \phi^T dA$$

$$\begin{bmatrix} M & & \\ & M & \\ & & M \end{bmatrix} \begin{Bmatrix} \frac{\partial u^n}{\partial t} \\ \frac{\partial v^n}{\partial t} \\ \frac{\partial H^n}{\partial t} \end{Bmatrix} + \begin{bmatrix} K & -fM & G_x \\ fM & K & G_x \\ -C_x & -C_y & O \end{bmatrix} \begin{Bmatrix} u^n \\ v^n \\ H^n \end{Bmatrix} + \begin{Bmatrix} F_x \\ F_y \\ F_H \end{Bmatrix} = \begin{Bmatrix} 0 \\ 0 \\ 0 \end{Bmatrix} \quad (3.14)$$

or in the abbreviated form

$$MQ + KQ = F \quad (3.15)$$

Then, all such elements must be assembled and the boundary conditions applied. Two different time integration procedures were used. The first one an implicit scheme involving the tapezoidal rule. Assume

$$\begin{aligned} \dot{Q} &= \frac{Q_T - Q_0}{\Delta t} \\ Q &= \frac{Q_T + Q_0}{2} \\ F &= \frac{F_0 + F_t}{2} \end{aligned} \quad (3.16)$$

Then eq (3.15) becomes

$$\left( \frac{2}{\Delta t} M + K \right) Q_t = (F_0 + F_t) + \left( \frac{2M}{\Delta t} - K \right) Q_0 \quad (3.17)$$

This can be written in the abbreviated form as

$$K^* Q_t = F^* \quad (3.18)$$

Then, the recurrence relationship is given by

$$Q = \left( K^* \right)^{-1} F^* \quad (3.19)$$

The  $K^*$  matrix which must be inverted will generally be a large asymmetrical banded matrix of size approximately three times the number of nodes by six times the element band width (i.e. the maximum difference between element nodal point numbers plus one). The explicit time integration used here follows the fourth-order Runge-Kutta method.

HAMBLIN (1976) and WILLIAMSON (1999) used finite-element techniques to study seiches, circulation and storm surges in Lake Winnipeg. His paper will be considered in some detail below. With reference to a Cartesian coordinate system (x, y) directed towards east and north, respectively, for a homogeneous fluid, under the hydrostatic approximation, with the neglect of the nonlinear terms and assuming a uniform value for the Coriolis parameter  $f$ :

$$\begin{aligned}
 \frac{\partial u}{\partial t} - fv + g \frac{\partial h}{\partial x} &= 0 \\
 \frac{\partial v}{\partial t} + fu + g \frac{\partial h}{\partial y} &= 0 \\
 \frac{\partial h}{\partial t} + \frac{\partial}{\partial x}(Du) + \frac{\partial}{\partial y}(Dv) &= 0
 \end{aligned} \tag{3.20}$$

where  $u$  and  $v$  are the vertically averaged horizontal velocity components in the  $x$  and  $y$  directions,  $D(x, y)$  is the water depth, and  $h(x, y, t)$  is the deviation of the water level from its equilibrium position.

Since we are concerned with periodic motion, the explicit time dependence can be eliminated by using an exponential time factor in the investigation of seiches. Then, the modified set of equations in (3.20) can be written using an elliptical operator (self-adjoint) for all boundary conditions (except when energy radiates through the openings). A variational formulation of the problem may be made and a numerical solution can be sought. For this, multiply the first equation of (3.20) by  $u^*$  ( $u^*$  is the complex conjugate of  $u$ ) and add this to the product of the second equation (3.20) of with  $v^*$ . Then, use the continuity equation, integrate over the volume of the lake, and use Green's theorem to give the total kinetic and potential energy in the lake:

$$I(h) = \int_A \left\{ hh^* + \frac{gD}{f^2 + \sigma^2} \left[ \frac{f}{i\sigma} \left( \frac{\partial h}{\partial y} \frac{\partial h^*}{\partial x} - \frac{\partial h}{\partial x} \frac{\partial h^*}{\partial y} \right) + \left( \frac{\partial h}{\partial x} \frac{\partial h^*}{\partial x} + \frac{\partial h}{\partial y} \frac{\partial h^*}{\partial y} \right) \right] \right\} dx dy \tag{3.21}$$

Where  $i = \sqrt{-1}$  and  $\sigma$  is the frequency of oscillation (i.e. seiche).

In deriving this equation, it is assumed that any of the following three boundary conditions can be used, noting that all of them permit zero energy flux across the boundaries: (a) vanishing depth at the shore line and finite values of  $h$  and its gradients, (b) finite depth at shoreline and zero velocity normal to the shoreline, and (c) finite depth and nonzero normal current but zero value of  $h$  across the boundary. HAMBLIN (1976) took zero depth at the coastline.

It can be shown that the function that minimizes eq. (3.21) will be the solution of eq. (3.20). The parameters  $h$  and  $h^*$  are expanded in a series of trial functions  $\Psi_i$  and weighting coefficients  $q_i'$ :

$$h = \sum_i q_i' \Psi_i \quad \text{and} \quad h^* = \sum_i q_i'^* \Psi_i^*$$

Substituting into eq. (3.21) gives

$$I(q'q'^*) = q'^{*T} \sigma^3 [L]q' + q'^{*T} \sigma [M]q' + q'^* [N]q' \tag{3.22}$$

Here,  $[L]$ ,  $[M]$ , and  $[N]$  are Hermitian matrices,  $q'$  is the vector of unknown coefficients, and  $q'^{*T}$  is the transpose of  $q'^*$ .

To determine the minimum of the approximating function:

$$\frac{\partial I}{\partial q^*} = 0$$

which gives form eq. (3.22)

$$\sigma^3 [L]z + \sigma [M]z + [N]z = 0 \quad (3.23)$$

where,  $z$  is the vector of weights minimizing  $I$ . The calculation of the approximating function proceeds as follows.

Lake Winnipeg is subdivided into triangular elements (Fig. 3.1a) giving a total of 144 elements. In the interior, the sides of the elements are straight lines, whereas at the coast they are curved. In locations where details are not important, a coarser grid has been used. The trial function is chosen such that the weighting coefficients become the free surface displacements,  $h$ , at the vertices and the three middle points (left side of Fig. 3.1b). Six points are required to determine the six coefficients of the second order polynomial in  $x$  and  $y$ . The quadratic surface determined in this manner is continuous across the edges between the triangles, but the gradients may not be continuous.

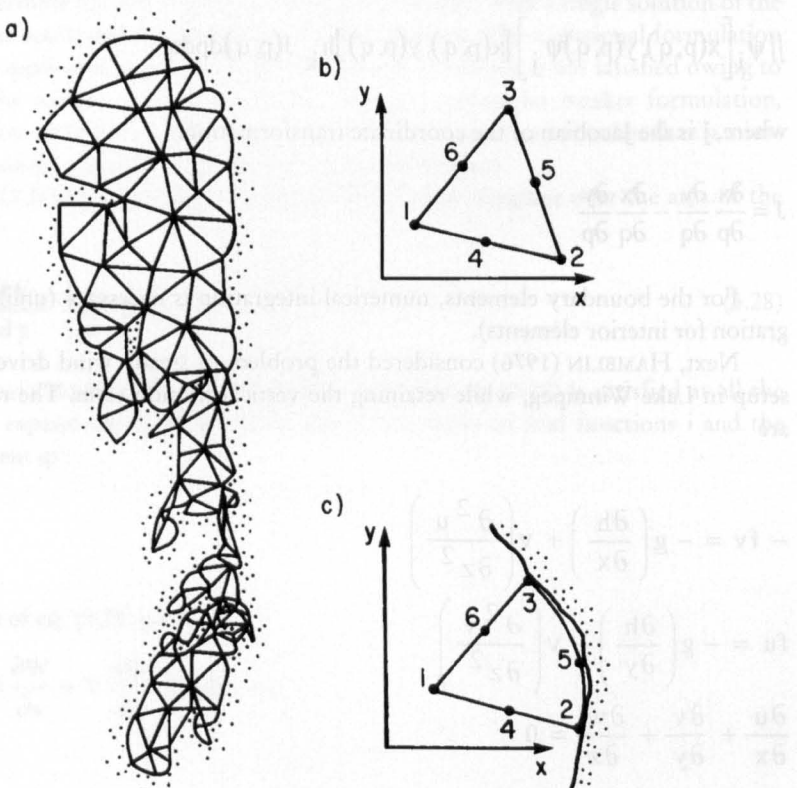


Fig. 3.1: (a) Triangular finite-element grid for Lake Winnipeg (144 elements); (b) a typical triangular element in the interior of the lake (the six nodes defining the element are numbered); (c) element adjacent to a boundary. (HAMBLIN, 1976)

Next, the depth  $D$  is expanded using an identical polynomial expression, in which the weighting coefficients become the specified depths at the six nodes of the triangle. If one expresses the Lagrangian interpolation functions in terms of the local triangular coordinates (rather than the global  $x$  and  $y$  coordinates), all the integrations in eq. (3.21) can be performed analytically for the interior elements. The matrices  $[L]$ ,  $[M]$ , and  $[N]$  are formed by summing the contributions from each element  $I$ . Owing to the symmetry of the variational formulation, the computer storage requirements and the number of integrations required are halved.

In general, the side of a triangle along the coastline will not coincide with the boundary (right side of Fig. 3.1b) and one must transform the curved shoreline into a straight line by means of a coordinate transformation. Define a coordinate system such that

$$x = x(p, q)$$

$$y = y(p, q)$$

Then, a boundary integration of the form

$$\iint \Psi_i(x, y) \Psi_j(x, y) h_k dx dy$$

becomes

$$\iint \Psi_i[x(p, q), y(p, q)] \Psi_j[x(p, q), y(p, q)] h_k J(p, q) dp dq \quad (3.21)$$

where,  $J$  is the Jacobian of the coordinate transformation:

$$J = \frac{\partial x}{\partial p} \frac{\partial y}{\partial q} - \frac{\partial x}{\partial q} \frac{\partial y}{\partial p}$$

For the boundary elements, numerical integration is necessary (unlike analytical integration for interior elements).

Next, HAMBLIN (1976) considered the problem of steady wind driven circulation and setup in Lake Winnipeg, while retaining the vertical friction term. The relevant equations are

$$\begin{aligned} -fv &= -g \left( \frac{\partial h}{\partial x} \right) + v \left( \frac{\partial^2 u}{\partial z^2} \right) \\ fu &= -g \left( \frac{\partial h}{\partial y} \right) + v \left( \frac{\partial^2 v}{\partial z^2} \right) \end{aligned} \quad (3.24)$$

$$\frac{\partial u}{\partial x} + \frac{\partial v}{\partial y} + \frac{\partial w}{\partial z} = 0 \quad (3.22)$$

where,  $w$  is the vertical eddy viscosity and  $w$  is the vertical component of the velocity (here,  $u$  and  $v$  are not vertically averaged).

The boundary conditions are the following:

$$v \left( \frac{\partial u}{\partial z} \right)_{z=0} = \frac{\tau_{sx}}{\rho} \quad \text{and} \quad v \left( \frac{\partial v}{\partial z} \right)_{z=0} = \frac{\tau_{sy}}{\rho} \tag{3.25}$$

where,  $\tau_{sx}$  and  $\tau_{sy}$  are the wind stress components at the surface and

$$u\xi_{z=-D} = 0 \quad \text{and} \quad v\xi_{z=-D} = -D = 0 \tag{3.26}$$

In the vertically integrated form the continuity equation is

$$\frac{\partial U}{\partial x} + \frac{\partial V}{\partial y} = 0 \tag{3.27}$$

where

$$(U, V) = \int_{-D}^0 (u, v) dz$$

is the horizontal transport vector. At the lateral boundaries the normal transport is taken as zero.

Making use of the Galerkin method, HAMBLIN (1976) developed a technique, which enables one to determine the free surface and transport variables with a single solution of the equations, which is applicable for multiple-connected regions. The variational formulation used earlier is not applicable because the self-adjointness condition is not satisfied owing to the presence of the surface wind stress terms. Hence, a somewhat weaker formulation, namely the Galerkin method, is used. In this method, a stationary point (rather than a minimum) of an expression related to the function will be determined.

Multiply eq. (3.27) by a weighting function  $W(x, t)$  and integrate over the area of the whole lake to give

$$\int W \left( \frac{\partial U}{\partial x} + \frac{\partial V}{\partial y} \right) dx dy = 0 \tag{3.28}$$

Using Galerkin's method,  $W$  must be chosen such that eq. (3.27) is satisfied at all the nodes. As above, expand the variables  $U, V,$  and  $h$  in a series of trial functions  $i$  and the weighting coefficient  $q_i$ :

$$h = \sum_i q_i \psi_i$$

Partial integration of eq. (3.28) gives

$$\oint W(\bar{v}d\bar{n}) - \iint \left( U \frac{\partial W}{\partial x} + V \frac{\partial W}{\partial y} \right) dx dy = 0$$

Note that the line integral is zero in the case where there is no river input or outflow. Using eq. (3.26) one can eliminate  $U$  and  $V$  and write

$$\begin{aligned} & \iint gD \left( E \frac{\partial h}{\partial x} - F \frac{\partial h}{\partial y} \right) \frac{\partial W}{\partial x} dx dy + \iint gD \left( F \frac{\partial h}{\partial x} + E \frac{\partial h}{\partial y} \right) \frac{\partial W}{\partial y} dx dy \\ &= - \iint \left[ C\tau_{s_x} - D\tau_{s_y} \right] \frac{\partial W}{\rho \partial x} dx dy - \iint \left[ A\tau_{s_x} + C\tau_{s_y} \right] \frac{\partial W}{\rho \partial x} dx dy \end{aligned} \quad (3.29)$$

(For details on the parameters  $C$ ,  $A$ ,  $E$  and  $F$ , see WELANDER (1957). In this section, Welander's parameter  $D$  has been replaced by  $A$ .)

For evaluating eq. (3.29) the parameters  $D$ ,  $C$ ,  $A$ ,  $E$ ,  $F$ ,  $\tau_{s_x}$  and  $\tau_{s_y}$  are expanded in a series of the same trial functions, i.e.:

$$\tau_{s_x} = \sum_i^6 \tau_{s_x i} \psi_i$$

Then, eq. (3.29) gives a system of six equations for each element:

$$\begin{aligned} & \sum_{j=1}^6 \iint gD \left( E \frac{\partial \psi_j}{\partial x} - F \frac{\partial \psi_j}{\partial y} \right) \frac{\partial \psi_i}{\partial x} dx dy + \iint gD \left( F \frac{\partial \psi_j}{\partial x} + E \frac{\partial \psi_j}{\partial y} \right) \frac{\partial \psi_i}{\partial y} dx dy \\ &= - \iint \left( C\tau_{s_x} - A\tau_{s_y} \right) \frac{\partial \psi_i}{\rho \partial x} dx dy - \\ & \iint \left( A\tau_{s_x} - C\tau_{s_y} \right) \frac{\partial \psi_i}{\rho \partial x} h_j dx dy \quad \text{for } i=1 \text{ to } 6 \end{aligned} \quad (3.30)$$

For the whole water body, the equations are obtained by successive integrations of each element and by adding all these, which assumes continuity of  $h_i$  at each node. The matrix

$$[M]h = B$$

is solved by Gaussian elimination.

Finally, HAMBLIN (1976) considered storm surges in Lake Winnipeg by beginning with the following time-dependent equations:

$$\begin{aligned} \frac{\partial u}{\partial t} - fv + g \frac{\partial h}{\partial x} &= \frac{\tau_{S_x}}{D\rho} + \frac{\tau_{B_x}}{D\rho} \\ \frac{\partial v}{\partial t} - fu + g \frac{\partial h}{\partial y} &= \frac{\tau_{S_y}}{D\rho} + \frac{\tau_{B_y}}{D\rho} \\ \frac{\partial h}{\partial t} + \frac{\partial}{\partial x} (Du) + \frac{\partial}{\partial y} (Dv) &= 0 \end{aligned} \quad (3.31)$$

where,  $\tau_B$  is the bottom stress.

HAMBLIN used a semianalytic technique (spectral method) in which the time variable is treated analytically and the space variables are treated numerically. Equations (3.31) can be written as in the finite element method as

$$\frac{dQ}{dt} = [M]Q + T(t) \tag{3.32}$$

where, the vector Q consists of the individual components of the current and h, the vector T consists of the wind stress components at each node, and the matrix [M] consists of coefficients which include f, g, D and the bottom friction.

For the initial condition, Q(0), the general solution of eq. (3.32) can be written as

$$Q(t) = [X(t)]Q(0) + \int_0^t [X(t-t')]T(t')dt' \tag{3.33}$$

where,

$$[X(t)] = [C] \begin{bmatrix} e^{\sigma_1 t} & & \\ & \ddots & \\ & & e^{\sigma_n t} \end{bmatrix} [C]^{-1}$$

Here,  $\sigma$  are the eigenvalues and [C] is the matrix of eigenvectors of

$$\{[M] - \sigma[I]\} \{C_i\} = 0$$

If the fluid body is initially at rest, Q(0) = 0 and a suddenly imposed wind stress can be written as T(t) = K. Integrating of eq. (3.33) gives

$$[Q(t)] = -[C] \begin{bmatrix} \frac{1}{\sigma_1} & & \\ & \ddots & \\ & & \frac{1}{\sigma_n} \end{bmatrix} [C]^{-1}K + [C] \begin{bmatrix} e^{\sigma_1 t} & & \\ \sigma_1 & & \\ & \ddots & \\ & & e^{\sigma_n t} \\ & & & \sigma_n \end{bmatrix} [C]^{-1}K \tag{3.34}$$

The first term in this equation can be shown to be  $[M]^{-1}K$ , which is the solution to the steady-state problem

$$[M]Q = K$$

The second term is a weighted sum of the free modes of oscillation of the discrete problem of order n:

$$\sum_i^n W_i \{C_i\} e^{\sigma_i t}$$

The transient response of the lake interpreted in this manner shows the connection between the general time-dependent problem and the steady-state seiche problems considered earlier.

Let the vector of the free surface displacements be denoted by  $S$  and let the eigenvectors,  $C_i$ , consist only of  $h$ ; then, eq. (3.34) can be approximated:

$$h(t) \sim S + \sum_i^{n'} W_i \{C_i\} e^{\sigma t}$$

Where the limit  $n'$  is a subset of the total  $n$  eigenvectors of  $[M]$ . Since the water body is at rest initially,  $h(0) = 0$ . Then

$$[C] W = S$$

noting that the imaginary part of  $S$  is zero. Since initially,  $u$  and  $v$  are zero, then

$$\left. \frac{\partial h}{\partial t} \right|_{t=0} = 0 \quad \text{and} \quad \left. \frac{\partial^2 h}{\partial t^2} \right|_{t=0} = 0$$

Hence,

$$[C] \sigma W = 0 \quad \text{and} \quad [C] \sigma^2 W = 0$$

From these equations the weighting coefficients may be determined by minimizing the square of the free surface deviation,  $h$ , at each node in the water body.

After obtaining the step function response,  $h$  may be calculated for a general time history of wind forcing using the convolution integral. The unit impulse response can be obtained by differentiation of the step function response. The free surface displacement,  $h$ , can be calculated by convoluting the wind input,  $T(t)$ , with  $h_{imp}$

$$h(t) = \int_0^t h_{imp}(t - t') T(t') dt'$$

In the discrete form, this can be written as

$$h_K = \Delta t \sum_{i=0}^j h_{imp}^i T_{K-i}$$

### 3.3 Development in the late 1970s and early 1980s

PLATZMAN (1979) paid particular attention to proper treatment of the multiconnected regions in finite-element models and applied these concepts to a study of the normal modes of the world ocean. PLATZMAN (1981) discussed the response characteristics of finite-element tidal models.

LYNCH and GRAY (1980b) developed a variable size triangular-grid finite-element model in which the boundary is permitted to deform. This technique is especially suitable for simulating the penetration of storm surges over land. Certain details of their earlier works lea-

ding to this model are contained in GRAY and LYNCH (1977, 1979), LYNCH (1980) and LYNCH and GRAY (1978, 1979, 1980a). Here, mainly the moving boundary model will be considered.

LYNCH and GRAY (1980b) used the Galerkin finite-element approach (for fixed boundaries) with certain modifications to the moving boundary problem. First, consider the fixed boundary problem. In their notation, the problem may be stated as

$$Lu = f \tag{3.35}$$

where, L is a differential operator with derivatives in space and time,  $u(X, t)$  is the unknown function,  $f(X, t)$  is the known forcing function, X is the set of independent space variables, and t is time. One can use an approximate solution  $(x, t)$  as

$$u \sim \hat{u} = \sum_{j=1}^N u_j(t) \phi_j(X) \tag{3.36}$$

where,  $\phi_j(X)$  are known basic functions.

Substituting eq. (3.36) into eq. (3.35) produces a nonzero residual  $r(X, t)$ :

$$L \cdot \hat{u} - f \equiv r(X, t) \tag{3.37}$$

The basic requirement in the Galerkin procedure is that the residual must be orthogonal to each of the basis functions  $\phi_i$ , i.e.:

$$\langle r(X, t), \phi_i \rangle = 0 \quad i = 1, \dots, N \tag{3.38}$$

where, angle brackets denote the inner product. It can be seen that eq. (3.38) forms a set of ordinary differential equations for the function  $u_j(t)$ .

For the moving boundary problem, the following modifications must be made to this procedure. The basis function  $\phi_j$  now becomes an implicit function of time because its value at any point depends on the location of the nodes (of a grid which is deforming):

$$\phi_j = \phi_j[X, X_b(t)] = \phi_j(X, t) \tag{3.39}$$

where, the node coordinates are denoted by  $X_b(t)$ . In eq. 3.38, the integration domain of the inner product changes in time. Thus, the equations becomes nonstationary and nonlinear, as can be seen, for example, from the fact that the mass matrix,  $\langle \phi_j, \phi_i \rangle$ , which multiplies the time derivative terms,  $du_j/dt$ , changes with time.

Next, an additional relation must be added for the node motion:

$$\frac{d}{dt} X_b(t) = V_b(t) \tag{3.40}$$

where,  $V_b$  is the velocity of node b. Generally, for the interior nodes  $V_b = 0$  and for the boundary nodes  $V_b = v_b$  where  $V_b$  is the velocity of the node and  $v_b$  is the fluid velocity at node b. Finally, eq. (3.36) must be replaced with

$$\hat{u}(X, t) = \sum_{j=1}^N u_j(t) \phi_j(X, t) \tag{3.41}$$

where,  $u_j(t)$  is the value of  $\cdot$  at node j (i.e. at the moving joint,  $X_j(t)$ ).

The time derivatives of  $(X, t)$  will have, as expected, additional terms (underlined> not contained in a fixed boundary model:

$$\frac{\partial \hat{u}}{\partial t} = \sum_{j=1}^N \frac{du_j}{dt} \phi_j + \sum_{j=1}^N u_j \frac{d\phi_j}{dt} \quad (3.42)$$

and

$$\frac{\partial^2 \hat{u}}{\partial t^2} = \sum_{j=1}^N \frac{d^2 u_j}{dt^2} \phi_j + 2 \sum_{j=1}^N \frac{du_j}{dt} \frac{\partial \phi_j}{\partial t} + \sum_{j=1}^N u_j \frac{\partial^2 \phi_j}{\partial t^2} \quad (3.43)$$

Since the spatial domain is changing with time, the terms  $\partial \phi_j / \partial t$  and  $\partial^2 \phi_j / \partial t^2$  must be defined throughout the domain. Since these terms depend exclusively on the node locations  $X_i(t)$  and their derivatives, in principle one can write expressions for  $\partial \phi_j / \partial t$  and  $\partial^2 \phi_j / \partial t^2$ . However, since this is a tedious procedure, LYNCH and GRAY (1980b) developed an alternate procedure, which is applicable to any isoparametric element. For any two-dimensional isoparametric element, let  $x$  and  $y$  represent the global coordinates and  $\xi$  and  $\eta$  represent the local coordinates. It is convenient to transform this element from the global domain (in which it may have an irregular shape) to the local domain in which it will always have the shape of a square (in the  $\xi, \eta$ ) domain the basis functions depend only on  $\xi$  and  $\eta$ ). Since the  $(\xi, \eta)$  space does not deform, a basis function  $\phi(\xi, \eta)$  at a location  $(\xi_0, \eta_0)$  will not change with time. The corresponding location to  $(\xi_0, \eta_0)$  in the  $(x, y)$  domain, however, may change with time and it depends on the isoparametric transformation:

$$X(t) = \sum_{i=1}^N X_i(t) \phi_i(\xi, \eta)$$

From this at a given point  $(\xi, \eta)$ :

$$\frac{dX}{dt} = \sum_{i=1}^M \frac{dX_i}{dt} \phi_i(\xi, \eta) = \sum_{i=1}^M V_i(t) \phi_i(\xi, \eta) = V^e \quad (3.44)$$

Where  $V^e$  is the elemental velocity (i.e. the velocity with which the element is moving). In a reference frame, which is moving with the elemental velocity, there is no change in  $\phi_i$ , and one can write

$$\frac{d\phi_i}{dt} = \frac{\partial \phi_i}{\partial t} + V^e \nabla \phi_i = 0 \quad (3.45)$$

Similarly, one can write

$$\frac{\partial^2 \phi_i}{\partial t^2} = - \left[ \sum_{i=1}^M \frac{dV_i}{dt} \phi_j \right] \nabla \phi_i + 2V^e (\nabla V^e) \nabla \phi_i + V^e (\nabla \nabla \phi_i) V^e \quad (3.46)$$

LYNCH and GRAY (1979) showed that, for the shallow-water problem, rather than using the continuity equation in its ordinary form, a computationally superior way is to use the following wave equation, which can be derived from the momentum and continuity equations:

$$\frac{\partial^2 H}{\partial t^2} + \tau \frac{\partial H}{\partial t} = \nabla (g H \nabla \zeta) + H V (\nabla \tau) + \nabla [\nabla (H V V) + f X H V - W] \quad (3.47)$$

This has to be integrated in time together with the horizontal momentum equation

$$\frac{\partial \mathbf{V}}{\partial t} = -\nabla \nabla V - f \mathbf{X} \mathbf{V} - g \nabla \zeta - \tau \mathbf{v} + \frac{\mathbf{W}}{H} \tag{3.48}$$

where,  $H(\mathbf{X}, t)$  is the total depth,  $\zeta(\mathbf{X}, t)$  is the free surface perturbation,  $h(\mathbf{X})$  is the equilibrium water depth,  $\mathbf{V}(\mathbf{X}, t)$  is the horizontal velocity vector (vertically averaged),  $f$  is the Coriolis parameter,  $g$  is gravity, and  $\mathbf{W}(\mathbf{X}, t)$  is the wind stress. The bottom stress is written as

$$\tau \mathbf{v}(\mathbf{X}, t) = \frac{g |\mathbf{V}| \mathbf{V}}{C^2 H} \tag{3.49}$$

where,  $C(\mathbf{X}, t)$  is the Chezy coefficient.

The boundary condition is

$$H = 0 \text{ on } \mathbf{X} = \mathbf{X}_0 + \int_0^t \mathbf{V} dt \tag{3.50}$$

Where  $\mathbf{X}(t)$  is the location of the boundary at time  $t$ ,  $\mathbf{X}_0$  is the initial time position of the boundary,  $\mathbf{V}$  is the velocity of the boundary, and  $\mathbf{v}$  is the velocity of the fluid.

Solutions of eq. (3.47) and (3.48) can be written in the finite-element form as follows:

$$\begin{aligned} H(\mathbf{X}, t) &\sim \sum_{j=1}^N H_j(t) \phi_j(\mathbf{X}, t) \\ \mathbf{V}(\mathbf{X}, t) &\sim \sum_{j=1}^N \mathbf{V}_j(t) \phi_j(\mathbf{X}, t) \\ \tau(\mathbf{X}, t) &\sim \sum_{j=1}^N \tau_j(t) \phi_j(\mathbf{X}, t) \end{aligned} \tag{3.51}$$

Substituting eq. (3.51) into eq. (3.47) and (3.48) and equating the weighted residuals to zero gives the following set of ordinary differential equations:

$$\begin{aligned} \sum_{j=1}^N \left( \frac{d^2 H_j}{dt^2} \langle \phi_j, \phi_i \rangle + 2 \frac{dH_j}{dt} \langle \frac{\partial \phi_j}{\partial t}, \phi_i \rangle + H_j \left\langle \frac{\partial^2 \phi_j}{\partial t^2}, \phi_i \right\rangle \right. \\ \left. + \frac{dH_j}{dt} \langle \tau \phi_j, \phi_i \rangle + H_j \left\langle \pi \frac{\partial \phi_j}{\partial t}, \phi_i \right\rangle \right) = \langle R_w, \phi_i \rangle \end{aligned} \tag{3.52}$$

and

$$\sum_{j=1}^N \left( \frac{d\mathbf{V}_j}{dt} \langle \phi_j, \phi_i \rangle + \mathbf{V}_j \langle \frac{\partial \phi_j}{\partial t}, \phi_i \rangle \right) = \langle R_M, \phi_i \rangle, i = 1, \dots, N \tag{3.53}$$

Here  $R_w(\mathbf{X}, t)$  and  $R_M(\mathbf{x}, t)$  are the right sides of eq. (3.47) and (3.48), respectively.

For the time derivative terms, a standard three-level finite-difference scheme has been used. For a stationary grid and one-dimensional case the C-F-L stability criterion reduces to

$$gH \left( \frac{\Delta t}{\Delta x} \right)^2 \leq \frac{1}{3} \quad (3.54)$$

The boundary condition  $v = v$  (i. e. fluid velocity equals the velocity of boundary movement) may lead to significant shearing of the boundary elements. To avoid this, LYNCH and GRAY (1980b) satisfied the mass conservation by requiring that

$$H = 0 \quad \text{or} \quad X = X_0 + \int_0^t V dt \quad (V - v)n = 0 \quad (3.55)$$

Where  $n$  is a unit vector normal to the boundary. Rather than attempting to satisfy this relation at every boundary grid point, one can satisfy it in an average sense by requiring that

$$\int_S (V - v)n dS = 0 \quad (3.56)$$

Using the finite-element solution forms for  $V$  and  $v$ :

$$V \sim \sum_i V_i \phi_i \quad (3.57)$$

$$v \sim \sum_i v_i \phi_i$$

Substituting eq. 3.57 into 3.56 gives

$$\sum_i \int_S (V_i - v_i)n \phi_i dS = 0 \quad (3.58)$$

To obtain an expression for the local normal direction that each term of eq. (3.58) be zero, i.e.:

$$(V_i - v_i) \int_S n \phi_i dS = 0 \quad (3.59)$$

From this one can define the modal normal direction,  $n_i$ , as follows:

$$n_i \equiv \frac{\int_S n \phi_i dS}{\left| \int_S n \phi_i dS \right|} \quad (3.60)$$

where, node  $i$  represent the junction of two moving segments of the boundary. Using the divergence theorem:

$$\int_S n \phi_i dS = \iint_A \nabla \phi_i dA \quad (3.61)$$

where,  $A$  is the total domain. The moving boundary condition becomes, finally,

$$H_i = 0 \quad \text{on} \quad X_i = X_{i,0} + \int_0^t V_i dt, \quad (V_i - v_i)n_i = 0 \tag{3.62}$$

$$V_i \lambda_i = 0$$

where,  $i$  represent all moving boundary nodes. Here,  $\lambda_i$  is the tangential direction at node  $\lambda_i$ . The second relation in eq. (3.62) is invoked to reduce element shearing.

A typical time step proceeds as follows.

- 1) Using eq. (3.60) and based on the existing grid, the nodal normal directions are determined.
- 2) The nodal velocities at the boundary are determined eq. (3.62). The locations of the nodes are calculated from the following finite-difference from of the first relation in eq. (3.62).

$$X_{i,t+\Delta t} \sim X_{i,t-\Delta t} + 2\Delta t V_{i,t} \tag{3.63}$$

- 3) The term  $dV_i/dt$  (which is required to evaluate  $\partial^2\phi / \partial t^2$  is calculated from

$$\frac{dV_i}{dt} = \frac{d^2X_i}{dt^2} \sim \frac{X_{i,t+\Delta t} - 2X_{i,t} + X_{i,t-\Delta t}}{(\Delta t)^2} \tag{3.64}$$

- 4) From eq. (3.52) and (3.53)  $H_i$  and  $V_i$  are calculated at  $t + \Delta t$ . Then steps are repeated by beginning with the determination of the nodal normals.

### 3.4 The Corps of Engineers Models

In a series of reports and papers (BLAIN, 1997; CIALONE, 1991; LUETTICH et al., 1991, 1992; MARK and SCHEFFNER, 1993; SCHEFFNER et al., 1994; WESTERINK et al., 1992, 1993a, 1993b) the so-called “ADCIRC” model of the U.S. Army Corps of Engineers has been described. The following material is based on (WESTERINK et al., 1993b). “ADCIRC” stands for “An advanced three-dimensional circulation model for shelves, coasts and estuaries”. The ADCIRC – 2DDI is a depth-integrated option of a system of two and three-dimensional hydrodynamic codes of “ADCIRC”.

ADCIRC – 2DDI uses the depth-integrated equations of mass and momentum conservation, subject to the incompressibility, Boussinesq, and hydrostatic pressure approximations. Using the standard quadratic parameterization for bottom stress and neglecting baroclinic terms and lateral diffusion/dispersion effects leads to the following set of conservation statements in primitive non-conservative form expressed in a spherical coordinate system (FLATHER, 1988; KOLAR et al., 1994):

$$\frac{\partial \zeta}{\partial t} + \frac{1}{R \cos \varphi} \left[ \frac{\partial UH}{\partial \lambda} + \frac{\partial (VH \cos \varphi)}{\partial \varphi} \right] = 0 \tag{3.65}$$

$$\begin{aligned} \frac{\partial U}{\partial t} + \frac{1}{R \cos \varphi} U \frac{\partial U}{\partial \lambda} + \frac{1}{R} V \frac{\partial U}{\partial \varphi} - \left( \frac{\tan \varphi}{R} U + f \right) V = \\ - \frac{1}{R \cos \varphi} \frac{\partial}{\partial \lambda} \left[ \frac{p_s}{\rho_0} + g(\zeta - \eta) \right] + \frac{\tau_{s\lambda}}{\rho_0 H} + -\tau_* U \end{aligned} \tag{3.66}$$

$$\frac{\partial V}{\partial t} + \frac{1}{R \cos \varphi} U \frac{\partial V}{\partial \lambda} + \frac{1}{R} V \frac{\partial V}{\partial \varphi} + \left( \frac{\tan \varphi}{R} U + f \right) U = -\frac{1}{R} \frac{\partial}{\partial \varphi} \left[ \frac{p_s}{\rho_0} + g(\zeta - \eta) \right] + \frac{\tau_{s\varphi}}{\rho_0 H} + -\tau_* V \quad (3.67)$$

where

$t$  = time

$\lambda, \varphi$  = degrees longitude (east of Greenwich positive) and degrees latitude (north of the equator positive)

$\zeta$  = free surface elevation relative to the geoid

$U, V$  = depth-averaged horizontal velocities

$R$  = radius of the earth

$H = \zeta + h$  = total water column

$h$  = bathymetric depth relative to the geoid

$f = 2 \Omega \sin \varphi$  = Coriolis parameter

$\Omega$  = angular speed of the earth

$p_s$  = atmospheric pressure at the free surface

$g$  = acceleration due to gravity

$\eta$  = effective Newtonian equilibrium tide potential

$\rho_0$  = reference density of water

$\tau_{s\lambda}, \tau_{s\varphi}$  = applied free surface stress

$$\tau_* = C_f \frac{(U^2 + V^2)^{1/2}}{H}$$

$C_f$  = bottom friction coefficient

A practical expression for the effective Newtonian equilibrium tide potential as given by REID (1990) is:

$$\eta(\lambda, \varphi, t) = \sum_{n,j} \alpha_{jn} C_{jn} f_{jn}(t_0) L_j(\varphi) \cos \left[ \frac{2\pi(t-t_0)}{T_{jn} + j\lambda + V_{jn}(t_0)} \right] \quad (3.68)$$

where

$C_{jn}$  = constant characterizing the amplitude of tidal constituent  $n$  of species  $j$

$\alpha_{jn}$  = effective earth elasticity factor for tidal constituent  $n$  of species  $j$

$f_{jn}$  = time-dependent nodal factor

$V_{jn}$  = time-dependent astronomical argument

$j = 0, 1, 2$  = tidal species ( $j = 0$ , declinational;  $j = 1$ , diurnal;  $j = 2$ , semidiurnal)

$L_0 = 3 \sin^2 \varphi - 1$

$L_1 = \sin(2\varphi)$

$L_2 = \cos^2(\varphi)$

$\lambda, \varphi$  = degrees longitude and latitude, respectively

$t_0$  = reference time

$T_{jn}$  = period of constituent  $n$  of species  $j$

Values for  $C_{jn}$  are presented by REID (1990). The value for the effective earth elasticity factor is typically taken as 0.69 for all tidal constituents (SCHWIDERSKI, 1980; HENDERSHOTT, 1981) although its value has been shown to be slightly constituent dependent.

To facilitate an FE solution to equations (3.65)–(3.67), these equations are mapped from spherical form into a rectilinear coordinate system using a Carte Parallelogrammitique (CP) projection (PEARSON, 1990):

$$x' = R (\lambda - \lambda_0) \cos \varphi_0 \tag{3.69}$$

$$y' = R \varphi \tag{3.70}$$

where,  $\lambda_0, \varphi_0 =$  center point of the projection. Applying the CP projection to equations (3.65)–(3.67) gives the shallow-water equations in primitive non-conservative form expressed in the CP coordinate system:

$$\frac{\partial \zeta}{\partial t} + \frac{\cos \varphi_0}{\cos \varphi} \frac{\partial(UH)}{\partial x'} + \frac{1}{\cos \varphi} \frac{\partial(VH \cos \varphi)}{\partial y'} = 0 \tag{3.71}$$

$$\begin{aligned} \frac{\partial U}{\partial t} + \frac{\cos \varphi_0}{\cos \varphi} U \frac{\partial U}{\partial x'} + V \frac{\partial U}{\partial y'} - \left( \frac{\tan \varphi}{R} U + f \right) V = \\ - \frac{\cos \varphi_0}{\cos \varphi} \frac{\partial}{\partial x'} \left[ \frac{p_s}{\rho_0} + g(\zeta - \eta) \right] + \frac{\tau_s \lambda}{\rho_0 H} - \tau_* U \end{aligned} \tag{3.72}$$

$$\begin{aligned} \frac{\partial V}{\partial t} + \frac{\cos \varphi_0}{\cos \varphi} U \frac{\partial V}{\partial x'} + V \frac{\partial V}{\partial y'} - \left( \frac{\tan \varphi}{R} U + f \right) U = \\ - \frac{\partial}{\partial y'} \left[ \frac{p_s}{\rho_0} + g(\zeta - \eta) \right] + \frac{\tau_s \varphi}{\rho_0 H} - \tau_* V \end{aligned} \tag{3.73}$$

Utilizing the FE method to resolve the spatial dependence in the shallow-water equations in their primitive form gives inaccurate solutions with severe artificial near 2.  $\Delta$  However, reformulating the primitive equations into a GWCE (Generalized Wave Continuity Equation) form gives highly accurate, noise free, FE-based solutions to the shallow-water equations (LYNCH AND GRAY, 1979; KINNMARCK, 1984). The GWCE is derived by combining a time-differentiated form of the primitive continuity equation and a spatially differentiated form of the primitive momentum equations recast into conservative form, reformulating the convective terms into non-conservative form and adding the primitive form of the continuity equation multiplied by a constant in time and space,  $\tau_0$  (LYNCH and GRAY, 1979; LUETTICH et al., 1992). The GWCE in the CP coordinate system is:

$$\begin{aligned}
 & \frac{\partial^2 \zeta}{\partial t^2} + \tau_0 \frac{\partial \zeta}{\partial t} + \frac{\cos \varphi_0}{\cos \varphi} \frac{\partial}{\partial x'} \frac{\partial \zeta}{\partial t} \\
 & \left\{ U - \frac{\cos \varphi_0}{\cos \varphi} U_H \frac{\partial U}{\partial x'} - v_H \frac{\partial U}{\partial y'} + \left( \frac{\tan \varphi}{R} U + f \right) v_H - \right. \\
 & \left. H \frac{\cos \varphi_0}{\cos \varphi} \frac{\partial}{\partial x'} \left[ \frac{p_s}{\rho_0} + g(\zeta - \eta) \right] - (\tau_* - \tau_0) U_H + \frac{\tau_{s\lambda}}{\rho_0} \right\} \\
 & + \frac{\partial}{\partial y'} \left\{ v \frac{\partial \zeta}{\partial t} - \frac{\cos \varphi_0}{\cos \varphi} U_H \frac{\partial v}{\partial x'} - v_H \frac{\partial v}{\partial y'} - \right. \\
 & \left. \left( \frac{\tan \varphi}{R} U + f \right) U_H - \right. \\
 & \left. H \frac{\partial}{\partial y'} \left[ \frac{p_s}{\rho_0} + g(\zeta - \eta) \right] - (\tau_* - \tau_0) v_H + \frac{\tau_{s\varphi}}{\rho_0} \right\} \\
 & - \frac{\partial}{\partial t} \left( \frac{\tan \varphi}{R} v_H \right) + -\tau_0 \left( \frac{\tan \varphi}{R} v_H \right) = 0
 \end{aligned} \tag{3.74}$$

The GWCE (equation 3.74) is solved in conjunction with the primitive momentum equations in non-conservative form (equations 3.72 and 3.73).

The high accuracy of GWCE-based FE solutions is a result of their excellent numerical amplitude and phase propagation characteristics. In fact, Fourier analysis indicates that in constant depth water and using linear interpolation, a linear tidal wave resolved with 25 nodes per wavelength is more than adequately resolved over the range of Courant numbers ( $C = \sqrt{gh}\Delta t/\Delta x \leq 1.0$  (LUETTICH et al., 1992)). Furthermore, the monotonic dispersion behavior of GWCE-based FE solutions avoids generating artificial near 2.  $\Delta x$  modes, which plague primitive-based FE solutions (PLATZMAN, 1981; FOREMAN, 1983). The monotonic dispersion behavior of GWCE-based FE solutions are very similar to that associated with staggered finite difference solutions to the primitive shallow-water equations (WESTERINK and GRAY, 1991). GWCE-based FE solutions to the shallow-water equations allow for extremely flexible spatial discretizations, which result in a highly effective minimization of the discrete size of any problem, (FOREMAN, 1988).

The details of ADCIRC, the implementation of the GWCE-based solution to the shallow-water equations, are described by LUETTICH et al. (1992). As most GWCE-based FE codes, ADCIRC applies three-noded linear triangles for surface elevation, velocity and depth. Furthermore, the decoupling of the time and space discrete form of the GWCE and momentum equations, time-independent and/or tri-diagonal system matrices, elimination of spatial integration procedures during time-stepping, and full vectorization of all major loops results in a highly efficient code.

SCHEFFNER et al. (1994) used ADCIRC to simulate storm surges from hurricanes on the Gulf of Mexico and east coasts of U. S. A. Fig. 3.2 shows the finite element grid used in these simulations.

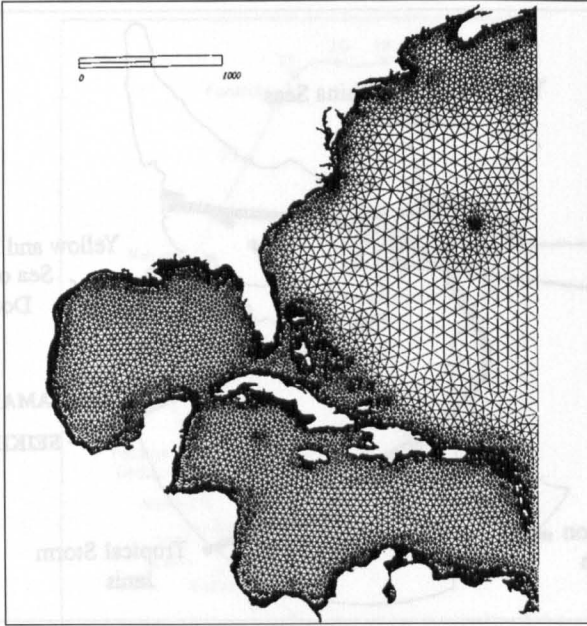


Fig. 3.2: The east coast, Gulf of Mexico, and Caribbean Sea computational domain. (SCHEFFNET et al., 1994).

BLAIN (1997) simulated hurricane generated storm surges on the coast of Florida and also for the coast of Northeast Asia. These model domains are respectively shown in Fig. 3.3 and 3.4.

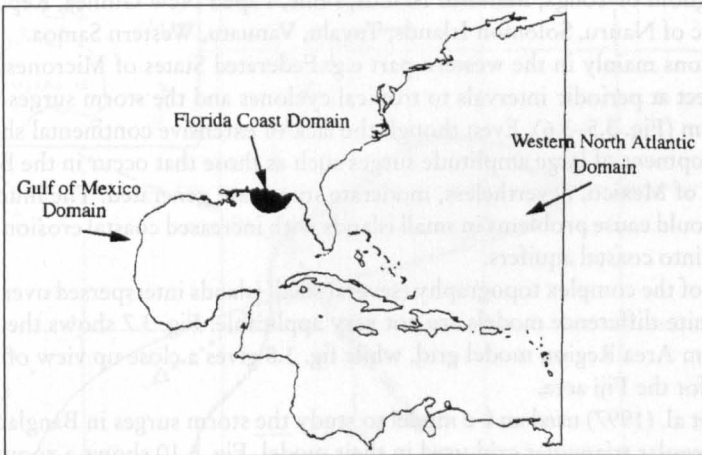


Fig. 3.3: Three domain sizes evaluated in the prediction of storm surge on the US Florida coast from hurricane Kate, 1985. (BLAIN, 1997).

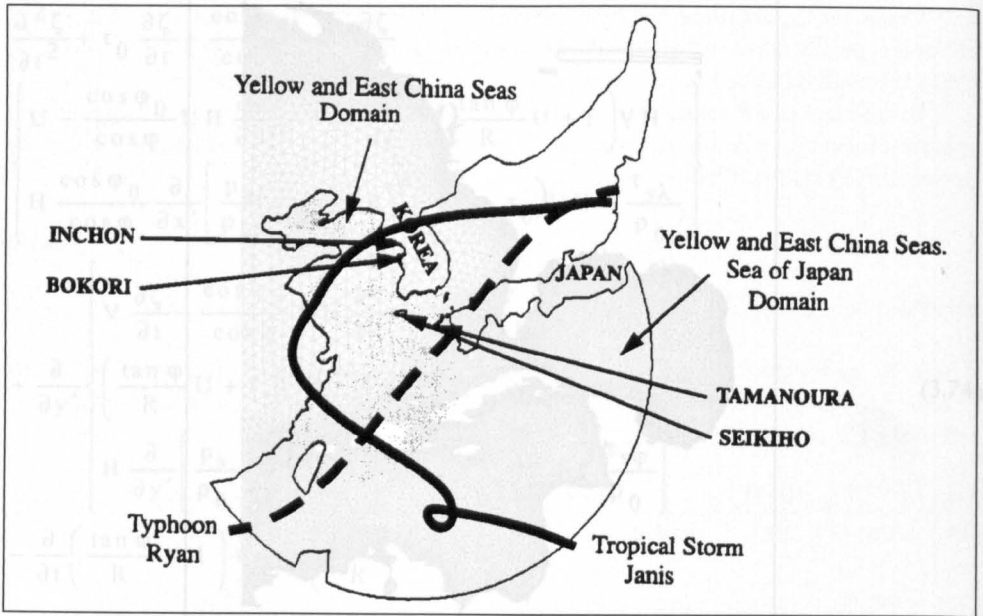


Fig. 3.4: Two domain sizes for the Yellow and East China Seas region, together with the paths of tropical storm Janis (August, 1995) and typhoon Ryan (September, 1995) and four hydrograph station locations. (BLAIN, 1997)

### 3.5 Other f-e Models

LUICK et al. (1997) studied storm surges in the Pacific forum region. The South Pacific region consists of the following island nations: Cook Islands, Federated States of Micronesia, Fiji, Kingdom of Tonga, Marshall Islands, Niue, Papua New Guinea, Republic of Kiribati, Republic of Nauru, Solomon Islands, Tuvalu, Vanuatu, Western Samoa.

The nations mainly in the western part e.g. Federated States of Micronesia (FSM) and Fiji, are subject at periodic intervals to tropical cyclones and the storm surges that are produced by them (Fig. 3.5–3.6). Even though the lack of extensive continental shelves precludes the development of large amplitude surges such as those that occur in the Bay of Bengal and the Gulf of Mexico, nevertheless, moderate surges are generated. The inundation from such surges could cause problems in small islands with increased coastal erosion and salt-water intrusion into coastal aquifers.

Because of the complex topography (several small islands interspersed over a large area), traditional finite-difference models are not very applicable. Fig. 3.7 shows the irregular triangular Forum Area Region model grid, while fig. 3.8 gives a close up view of irregular triangular grid for the Fiji area.

HENRY et al. (1997) used an f-e model to study the storm surges in Bangladesh. Fig. 3.9 shows the irregular triangular grid used in their model. Fig. 3.10 shows a zoom-in-view for the Meghna Estuary region. Fig. 3.11 and 3.12 respectively compare the computed and observed surges at Cox's Bazaar, Khepupara (April 1991 event). The discrepancies between the observed and computed surges could be mostly attributed to deficiencies in the prescribed meteorological input data.

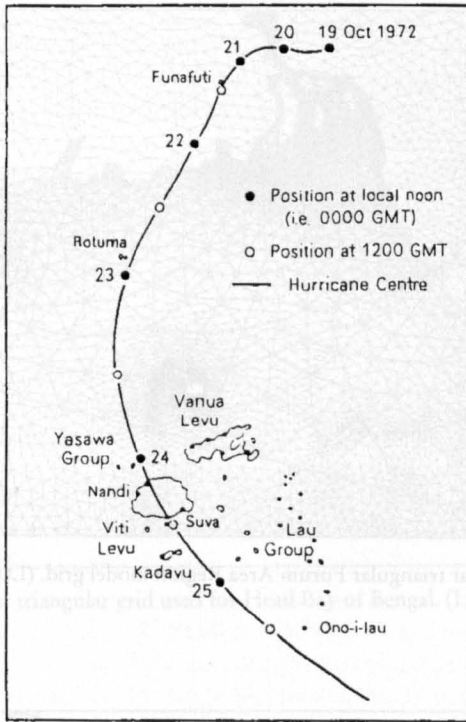


Fig. 3.5: Track of Hurricane Bebe October 1972 (from New Zealand Meteorological Service)

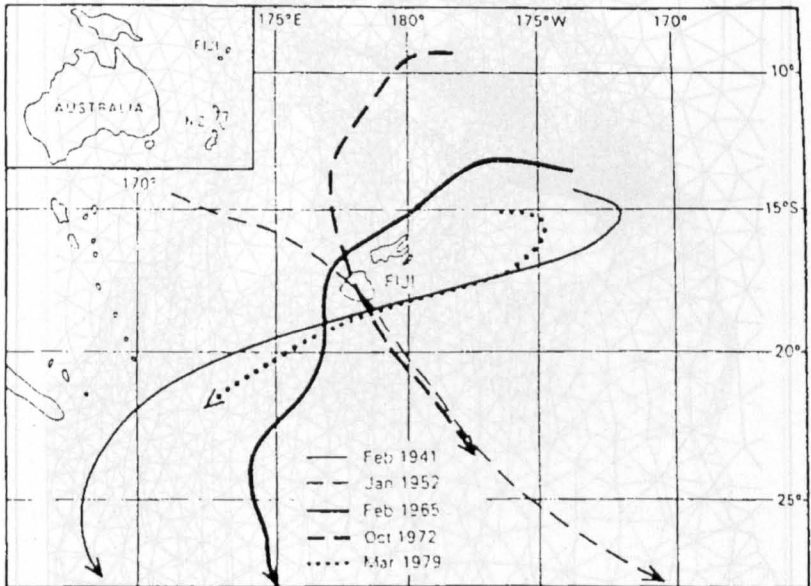


Fig. 3.6: Tracks of severe Hurricanes in Fiji area between 1940 and 1979 (from Fiji Meteorological Service)



Fig. 3.7: Irregular triangular Forum Area Region model grid. (LUICK et al., 1997)

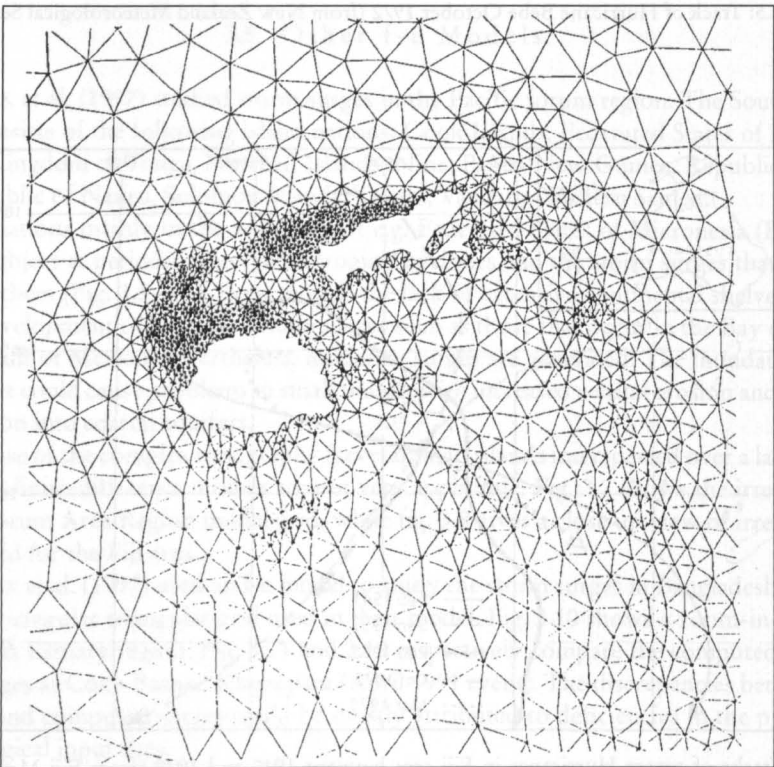


Fig. 3.8: Close up view of irregular triangular grid for the Fiji area. (LUICK et al., 1997)

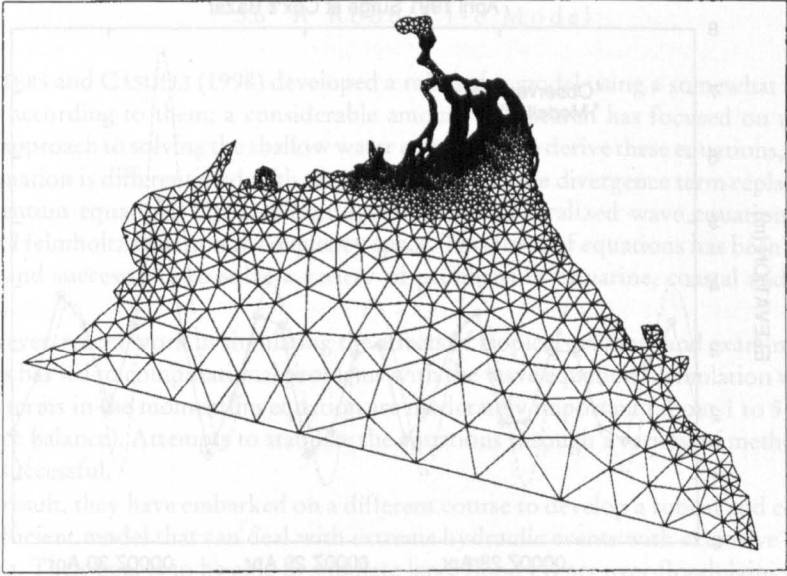


Fig. 3.9: Irregular triangular grid used for Head Bay of Bengal. (HENRY et al., 1997)

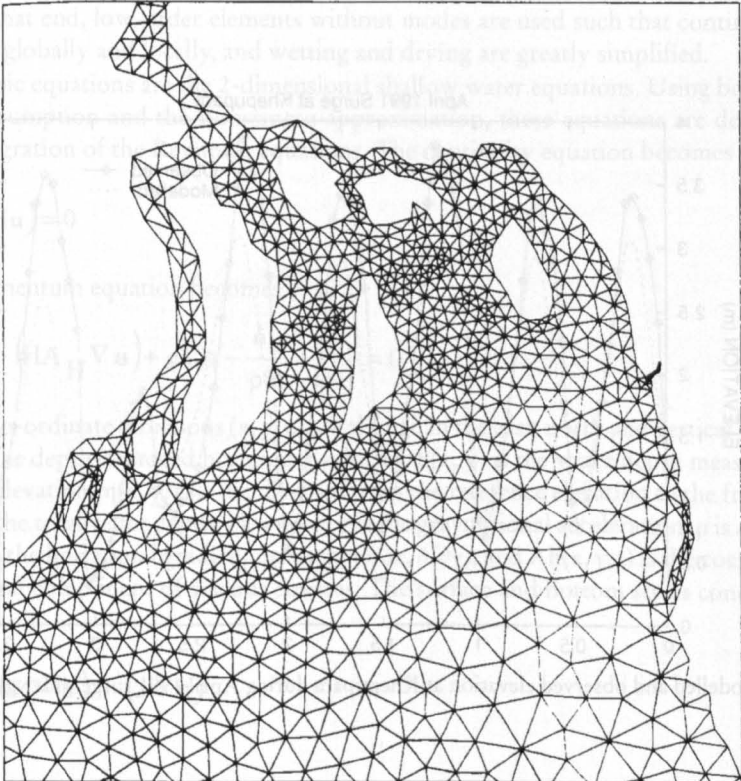


Fig. 3.10: Close up of part of grid covering Meghna Estuary. (HENRY et al., 1997)

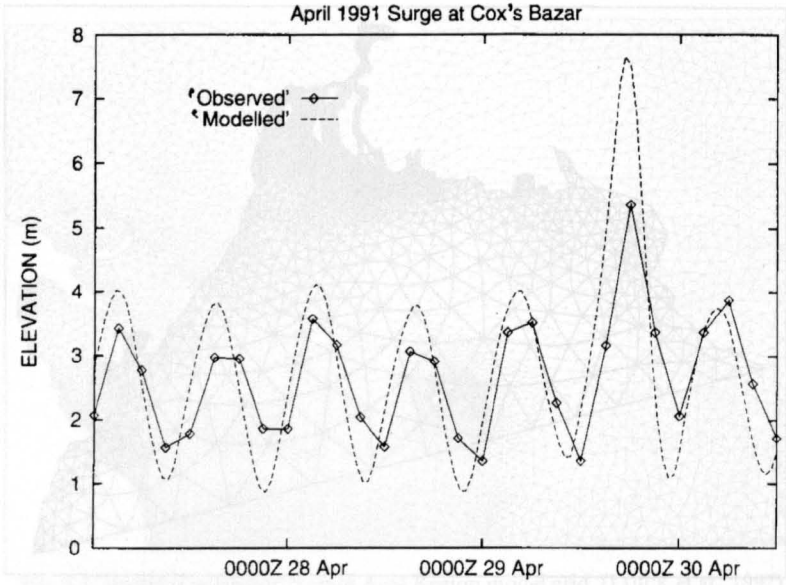


Fig. 3.11: Modelled and observed elevation at Cox's Bazaar during April 1991 surge. (HENRY et al., 1997)

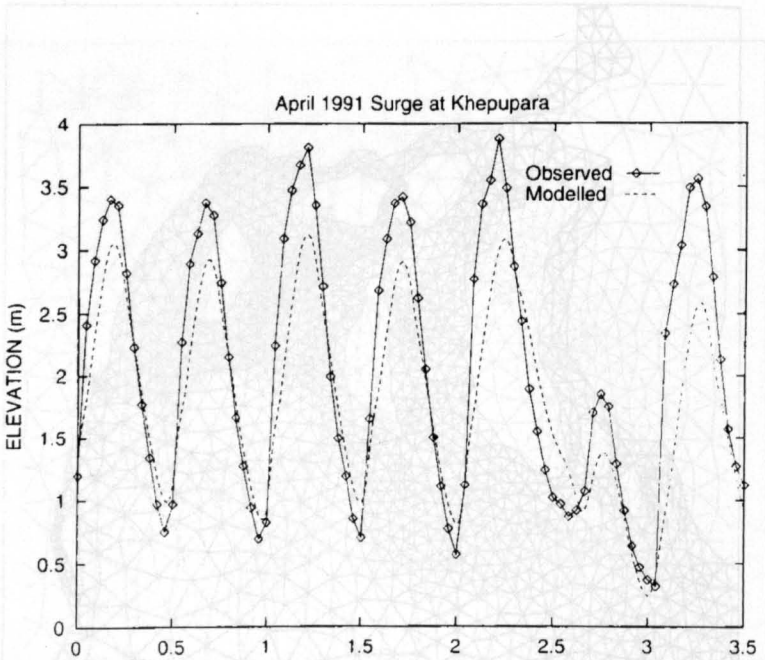


Fig. 3.12: Modelled and observed elevation at Khepupara during April 1991 surge. (HENRY et al., 1997)

### 3.6 A Robust f-e Model

WALTERS and CASULLI (1998) developed a robust f-e model using a somewhat different approach according to them; a considerable amount of research has focused on the wave equation approach to solving the shallow water equations. To derive these equations, the continuity equation is differentiated with respect to time, and the divergence term replaced with the momentum equation. The resultant equations are generalized wave equation in time space or a Helmholtz equation in frequency space. This form of equations has been used extensively and successfully to solve a variety of problems in estuarine, coastal and oceanic flows.

However, recent work in simulating the effects of tropical cyclones and examining river hydraulics has led to computational problems with the wave equation formulation when the advective terms in the momentum equation are moderately important (about 1 to 5 per cent of the force balance). Attempts to stabilize the equations through a variety of methods have not been successful.

As a result, they have embarked on a different course to develop a robust and computationally efficient model that can deal with extreme hydraulic events with extensive flooding and drying. Their goal is to be able to simulate large flood events over floodplains of variable extent.

The method adopted here is to use the primitive shallow water equations and form a wave equation at the discrete level. This procedure carries through the properties of the original discretized equations so that the use of elements without computational modes is essential. To that end, low-order elements without modes are used such that continuity is satisfied both globally and locally, and wetting and drying are greatly simplified.

The basic equations are the 2-dimensional shallow water equations. Using both the hydrostatic assumption and the Boussinesq approximation, these equations are derived by a vertical integration of the Reynolds equations. The continuity equation becomes

$$\frac{\partial \eta}{\partial t} + \nabla \cdot (H\mathbf{u}) = 0 \quad (3.75)$$

and the momentum equation becomes

$$\frac{d\mathbf{u}}{dt} - \frac{1}{H} \nabla \cdot (H\mathbf{A}_H \nabla \mathbf{u}) + g\nabla \eta - \frac{\hat{\delta}_s}{\rho H} + \frac{\hat{\delta}_b}{\rho H} = 0 \quad (3.76)$$

where, the co-ordinate directions ( $x, y, z$ ) are aligned in the east, north and vertical directions;  $\mathbf{u}(x, y, t)$  is the depth-averaged horizontal velocity;  $h(x, y)$  is the water depth measured from a reference elevation;  $\eta(x, y, t)$  is the distance from the reference elevation to the free surface;  $H(x, y, t)$  is the total water depth,  $H = \eta - h$ ;  $g$  is the gravitational acceleration;  $\rho$  is a reference density;  $\nabla$  is the horizontal gradient operator ( $\partial/\partial x, \partial/\partial y$ ); and  $A_h(x, y, t)$  is the coefficient for the horizontal component of viscous stresses. The surface and bottom stress conditions are given by

$$\frac{\hat{\delta}_s}{\rho} = \gamma_T H (\mathbf{u}_a - \mathbf{u}) \quad (z = \eta) \quad (3.77)$$

$$\frac{\hat{\delta}_b}{\rho} = C_D |\mathbf{u}| \mathbf{u} = \gamma_B H \mathbf{u} \quad (z = h) \quad (3.78)$$

where, the surface and bottom stress are denoted as  $\tau_s$  and  $\tau_b$  respectively,  $\mathbf{u}_a$  is the wind velocity, and  $C_D$  is a bottom drag coefficient. Essential boundary conditions on  $\eta$  or volumetric flux are set at open boundaries, and  $(\mathbf{u} \cdot \hat{\mathbf{n}}) = 0$  (no normal flow, where  $\hat{\mathbf{n}}$  is the unit normal) is set on land boundaries.

This study focuses on the solution for surface elevation in the two-dimensional, discrete wave equation form of the continuity equation and the solution for the horizontal velocity components in the momentum equation. The governing equations are approximated using standard Galerkin techniques. The equations are discretized after defining a set of 2-dimensional triangular elements in the horizontal plane. Mixed methods are used in such a way that the elements use a piecewise constant basis for  $\eta$  and a constant normal velocity on each edge.

The continuity equation (3.75) can be expressed in weighted residual form as: find  $\eta \in S$  such that

$$\int_{\Omega} \hat{\eta} \frac{\partial \eta}{\partial t} d\Omega + \int_{\Omega} \hat{\eta} \nabla \cdot (\mathbf{H} \mathbf{u}) d\Omega = 0, \quad \forall \hat{\eta} \in S \tag{3.79}$$

Here  $S$  is the space of square integrable functions and  $\Omega$  is the flow domain. Expanding  $\eta, \hat{\eta}$  in terms of the finite basis  $\phi$  and numerically integrating produces an algebraic problem for the nodal unknowns.

The weak form of momentum equation can be given as: find  $\mathbf{u} \in U$  such that

$$\int_{\Omega} \hat{\mathbf{u}} \left[ \frac{d\mathbf{u}}{dt} + \gamma_B \mathbf{u} - \gamma_T (\mathbf{u}_a - \mathbf{u}) - \nabla \cdot (\mathbf{A}_h \nabla \mathbf{u}) \right] d\Omega = - \int_{\Omega} \hat{\mathbf{u}} g \nabla \eta d\Omega, \quad \forall \hat{\mathbf{u}} \in U \tag{3.80}$$

where, the equation is interpreted component-wise and  $U$  is the space of vector functions that have a divergence. Note that the term  $(\nabla H/H)(\mathbf{A}_h \nabla \mathbf{u})$  arising from the expansion of the horizontal viscous stress term has been neglected. Expanding  $\mathbf{u}, \hat{\mathbf{u}}$  in terms of the finite element basis  $\phi$  again produces an algebraic problem for the nodal unknowns. The surface pressure gradient term and the horizontal stress term are integrated by parts to give

$$\begin{aligned} & \int_{\Omega} \hat{\mathbf{O}} \left[ \frac{d\mathbf{u}}{dt} + \gamma_B \mathbf{u} - \gamma_T (\mathbf{u}_a - \mathbf{u}) \right] d\Omega + \int_{\Omega} \nabla \hat{\mathbf{O}} \cdot (\mathbf{A}_h \nabla \mathbf{u}) d\Omega \\ & = \int_{\Omega} g \nabla \hat{\mathbf{O}} \eta d\Omega - \oint_{\Gamma} [g(\hat{\mathbf{O}} \eta) - \hat{\mathbf{O}} \mathbf{A}_h \nabla \mathbf{u} \cdot \hat{\mathbf{n}}] d\Gamma \end{aligned} \tag{3.81}$$

where,  $\Gamma$  is the boundary of the flow domain  $\Omega$ . The line integral in this equation provides a convenient means to specify the boundary conditions on  $\eta$  and horizontal stress.

These equations are discretized in time using a semi-implicit method such that the equations are evaluated in the time interval  $(\tau^m, \tau^{m+1})$ , where the superscript denotes the time level. The distance through the interval is given by the weight  $\theta$ . The semi-implicit approach is given as

$$\frac{\eta^{m+1} - \eta^m}{\Delta t} + \nabla \cdot \left[ \mathbf{H}^m \left( \theta \mathbf{u}^{m+1} + (1-\theta) \mathbf{u}^m \right) \right] = 0 \tag{3.82}$$

$$\frac{\mathbf{u}^{m+1} - \mathbf{u}^*}{\Delta t} + \theta \mathbf{G}^{m+1} + (1-\theta) \mathbf{G}^* = \mathbf{F}^* \tag{3.83}$$

$$\mathbf{G} = \gamma_B \mathbf{u} - \gamma_T (\mathbf{u}_a - \mathbf{u}) + g \nabla \eta \tag{3.84}$$

$$\mathbf{F}^* = \nabla \cdot (\mathbf{A}_h \nabla \mathbf{u})^* \tag{3.85}$$

Semi-Lagrangian methods are used in order to take advantage of the simplicity of Eulerian methods and the enhanced stability and accuracy of Lagrangian methods. Here the superscripts  $m$  and  $m+1$  denote variables evaluated at the fixed nodes in the Eulerian grid at times  $t^m$  and  $t^{m+1}$ . The subscript  $*$  denotes a variable evaluated at time  $t^m$  at the end of the Lagrangian trajectory from a computational node (see Fig. 3.13). At each time step, the velocity is integrated backwards with respect to time to determine where a particle would be at time  $t^m$  to arrive at a grid node at time  $t^{m+1}$ . The material derivative in equation (3.83), the first term, thus has a very simple form.

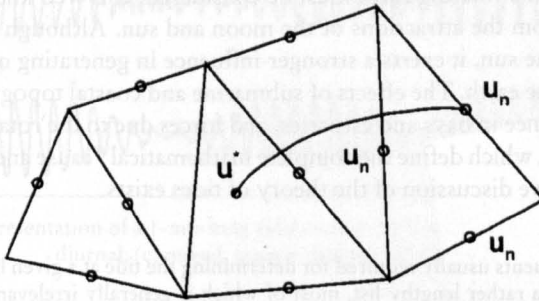


Fig. 3.13: Definition of the elements used and the Lagrangian trajectories. At time  $t^m$ , a particle starts at the location where velocity is  $u^*$ , and arrives at a node in the grid at time  $t^{m+1}$ . (WALTERS AND CASULLI, 1998)

There are three test problems studied (i) a simulation of tides in a polar quadrant region that indicates that there are no computational nodes; (ii) a simulation of tides in a regular channel with sloping bottom that provides an assessment of accuracy and convergence rate; and (iii) a simulation of a flood on the Big Lost River, Idaho, that assesses performance in a highly irregular but realistic geometry. The results look quite satisfactory.

KAWAHARA et al. (1982, 1983) used multi-level f-e models including stratification. Such models will be useful for the computation of currents associated with storm surges.

Three examples will be shown with this classification. First, a regular channel with sloping bottom, which is chosen such that the bottom is a constant that forces the constant level, which is chosen such that the bottom is a constant. The other two are chosen such that the bottom is a constant. The first example is a regular channel with sloping bottom, which is chosen such that the bottom is a constant. The second example is a regular channel with sloping bottom, which is chosen such that the bottom is a constant. The third example is a regular channel with sloping bottom, which is chosen such that the bottom is a constant.